Supporting Information

Selective CO_2–to–CO Photoreduction over Orthophosphate Semiconductor via Ag_3PO_4 Quantum Dots Decorated SnS_2 Nanosheets Direct Z-scheme Heterojunction

Fang-Yu Fu[a,b], Chi-Chan Fan[b,c], Mohammad Qorbani[b,d,*], Chih-Yang Huang[b,e,f,g], Ping-Chun Kuo[b,h], Jih-Shang Hwang[c], Guo-Jiun Shu[h], Sue-Min Chang[i], Heng-Liang Wu[b,d], Chih-I Wu[a,*], Kuei-Hsien Chen[b,e,*], Li-Chyong Chen[b,d,j,*]

[a] Graduate Institute of Photonics and Optoelectronics, National Taiwan University, Taipei 10617, Taiwan
[b] Center for Condensed Matter Sciences, National Taiwan University, Taipei 10617, Taiwan
[c] Institute of Optoelectronic Science, National Taiwan Ocean University, Keelung 202, Taiwan
[d] Center of Atomic Initiative for New Materials, National Taiwan University, Taipei 10617, Taiwan
[e] Institute of Atomic and Molecular Sciences, Academia Sinica, Taipei 10617, Taiwan
[f] Molecular Science and Technology Program, Taiwan International Graduate Program, Academia Sinica, Taipei 11529, Taiwan.
[g] International Graduate Program of Molecular Science and Technology, National Taiwan University, Taipei 10617, Taiwan.
[h] Department of Materials and Mineral Resources Engineering, National Taipei University of Technology, Taipei 106, Taiwan
[i] Institute of Environmental Engineering, National Yang Ming Chiao Tung University, Hsinchu 30010, Taiwan
[j] Department of Physics, National Taiwan University, Taipei 10617, Taiwan

*Corresponding authors:

E-mail addresses: mqorbani@ntu.edu.tw (M. Qorbani), chihiwu@ntu.edu.tw (C.-I Wu), chenkh@pub.iams.sinica.edu.tw (K.-H. Chen), and chenlc@ntu.edu.tw (L.-C. Chen)

Supporting Notes

Note S1. X-ray photoemission spectroscopy core level measurements. The following calculations were performed to determine the valence band offset (ΔE_v) of Ag_3PO_4/SnS_2 heterojunction [1]

$$\Delta E_v = |(E_{Sn3d_{5/2}}^{SnS_2} - E_{VBM}^{SnS_2}) - (E_{Ag3d_{5/2}}^{Ag_3PO_4} - E_{VBM}^{Ag_3PO_4}) - (E_{Sn3d_{5/2}}^{Ag_3PO_4/SnS_2} - E_{Ag3d_{5/2}}^{Ag_3PO_4/SnS_2})| \quad (1)$$

Where $E_{Sn3d_{5/2}}^{SnS_2}$ and $E_{Ag3d_{5/2}}^{Ag_3PO_4}$ are defined to a position of the core level at SnS_2 and Ag_3PO_4 interface, respectively. $E_{Sn3d_{5/2}}^{SnS_2} - E_{VBM}^{SnS_2}$ and $E_{Ag3d_{5/2}}^{Ag_3PO_4} - E_{VBM}^{Ag_3PO_4}$ terms depend on the binding energy difference between core level and valence band maximum. $E_{Sn3d_{5/2}}^{Ag_3PO_4/SnS_2} - E_{Ag3d_{5/2}}^{Ag_3PO_4/SnS_2}$ term was calculated for the potential of interface state within the SnS_2 and Ag_3PO_4 sampled region, thus this potential can correlate with the interface state or the sources of band bending at the heterointerface. First, the experimental determinations of X-ray photoemission spectroscopy (XPS) core level and VBM fitting results were presented in **Figure S8**. $E_{Sn3d_{5/2}}^{SnS_2} - E_{VBM}^{SnS_2}$ term was calculated to be 484.88 eV (*i.e.* 486.6-1.72). $E_{Ag3d_{5/2}}^{Ag_3PO_4} - E_{VBM}^{Ag_3PO_4}$ was calculated to be 366.25 eV (*i.e.* 367.9-1.65) and $E_{Sn3d_{5/2}}^{Ag_3PO_4/SnS_2} - E_{Ag3d_{5/2}}^{Ag_3PO_4/SnS_2}$ was calculated to be 118.20 eV (*i.e.*, 486.30-368.10). Accordingly, ΔE_v was calculated to be 0.43 eV (*i.e.* 484.88-366.25-118.20). Finally, the conduction band offset (ΔE_c) was derived from the bandgap values of SnS_2 (2.56 eV) and Ag_3PO_4 (2.47 eV), which were obtained from UV–visible spectra (**Figure 1a** in the main manuscript).

$$\Delta E_c = (E_g^{Ag_3PO_4} + \Delta E_v - E_g^{SnS_2}), \quad (2)$$

So, ΔE_c was determined to be 0.34 eV.

Supporting Figures

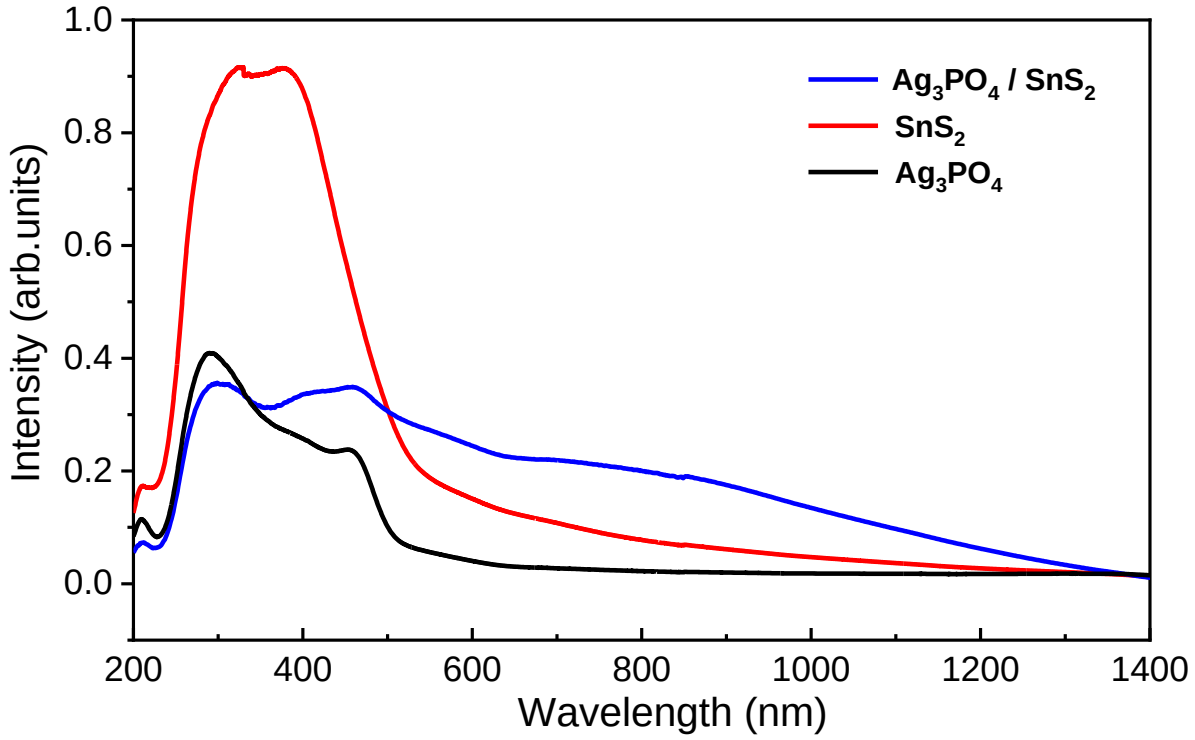

Figure S1. Non-normalized UV-vis absorption spectra of Ag_3PO_4, SnS_2 and Ag_3PO_4/SnS_2 samples

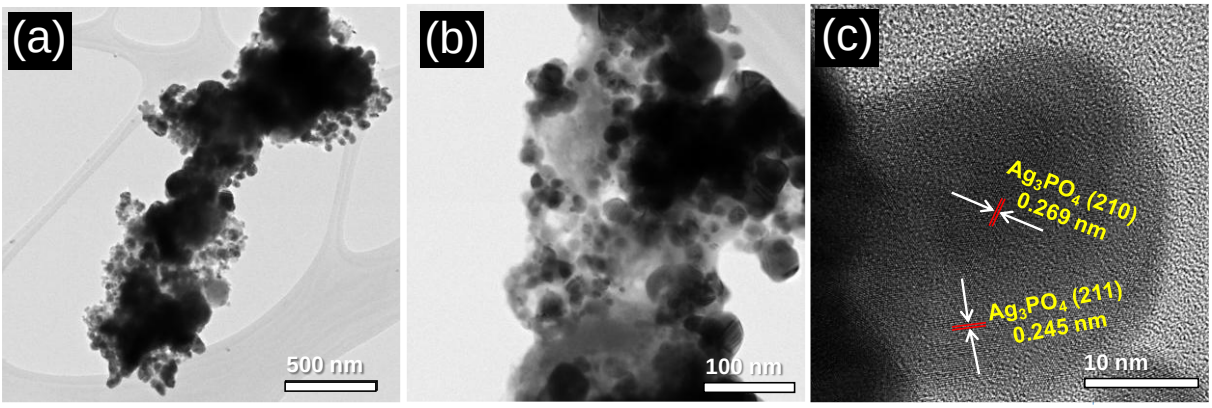

Figure S2. TEM images of Ag_3PO_4 with different magnifications (a) 15 kX, (b) 50 kX, and (c) 800 kX.

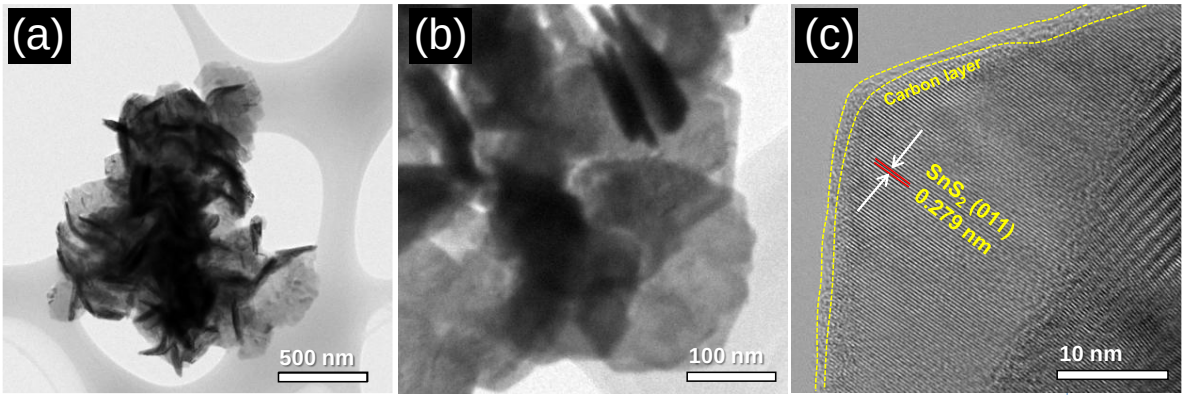

Figure S3. TEM images of SnS_2 with different magnifications (a) 15 kX, (b) 50 kX, and (c) 800 kX.

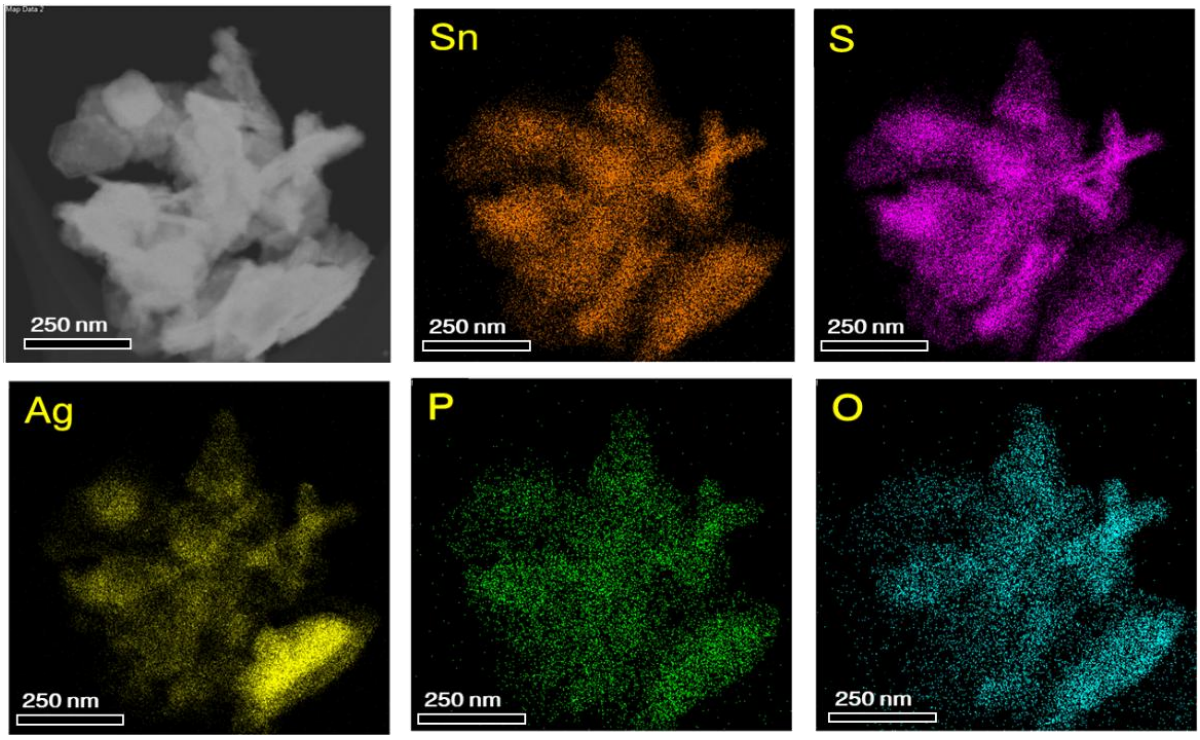

Figure S4. HAADF-STEM image and energy dispersive X-ray spectroscopy (EDS) elemental mapping of Sn, S, Ag, P, O for the Ag_3PO_4/SnS_2 sample.

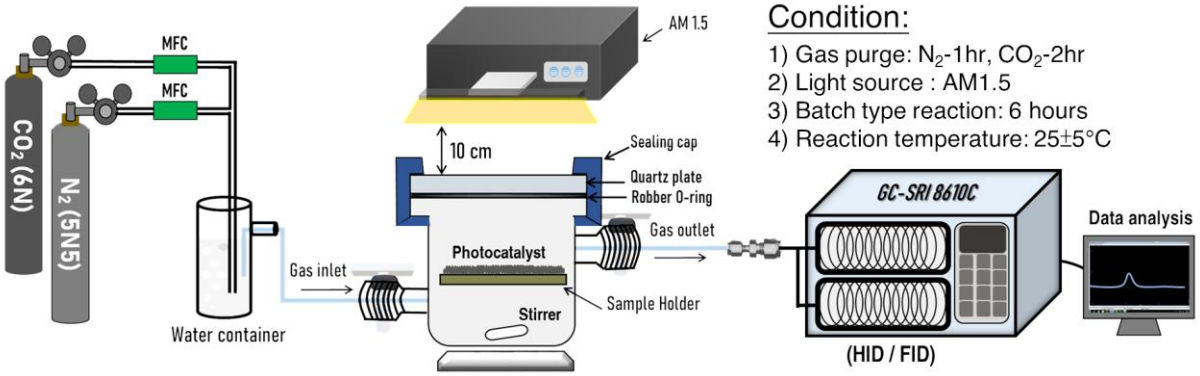

Figure S5. Schematic diagram of the gas-phase photocatalytic (PC) CO_2 reduction system.

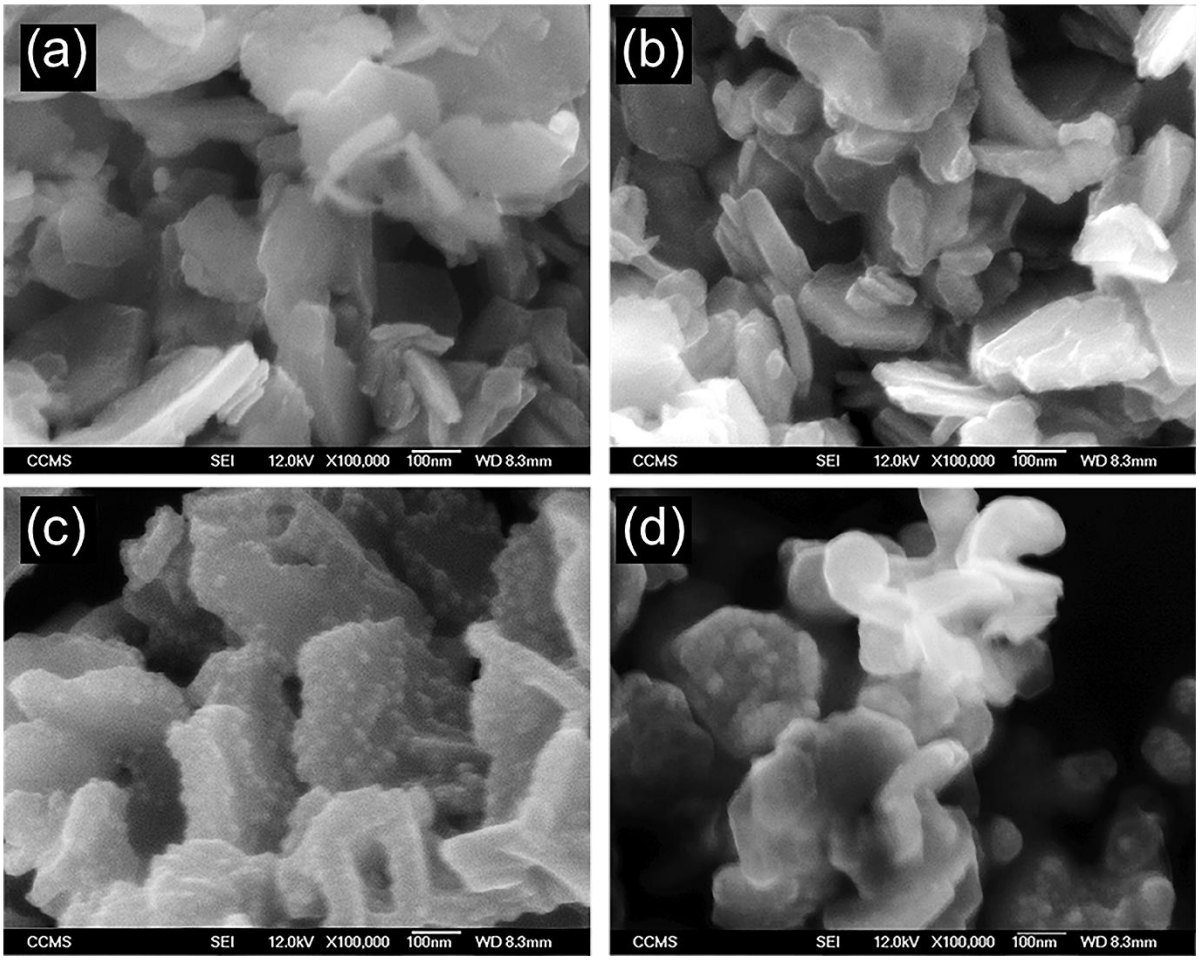

Figure S6. SEM images of the as-prepared Ag_3PO_4/SnS_2 heterostructures with different Ag_3PO_4–to–SnS_2 ratios. (a) 50–to–50, (b) 60–to–40, (c) 70–to–30, (d) 80–to–20.

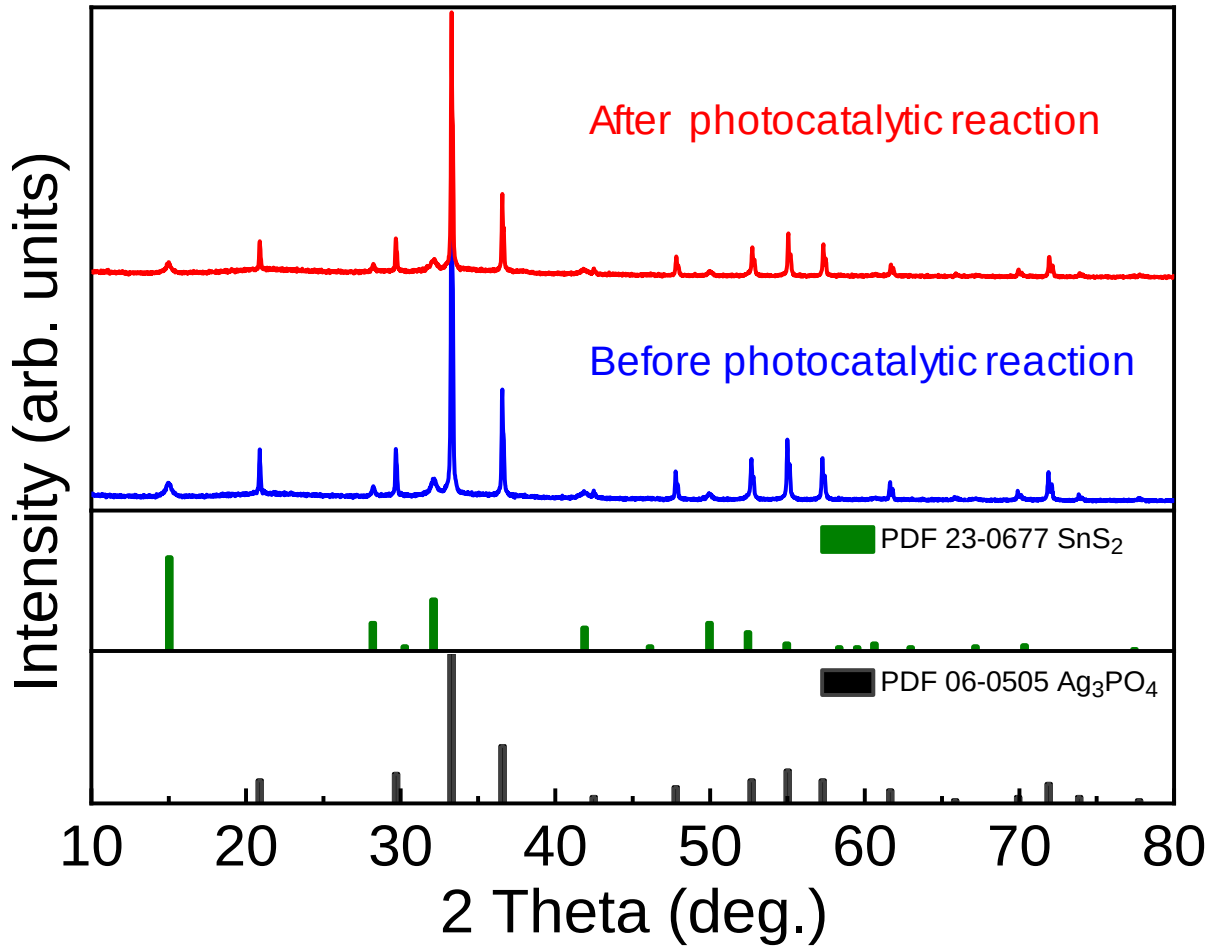

Figure S7. XRD patterns for the Ag_3PO_4/SnS_2 and the pristine Ag_3PO_4/SnS_2 sample after the photocatalytic CO_2 reduction stability test.

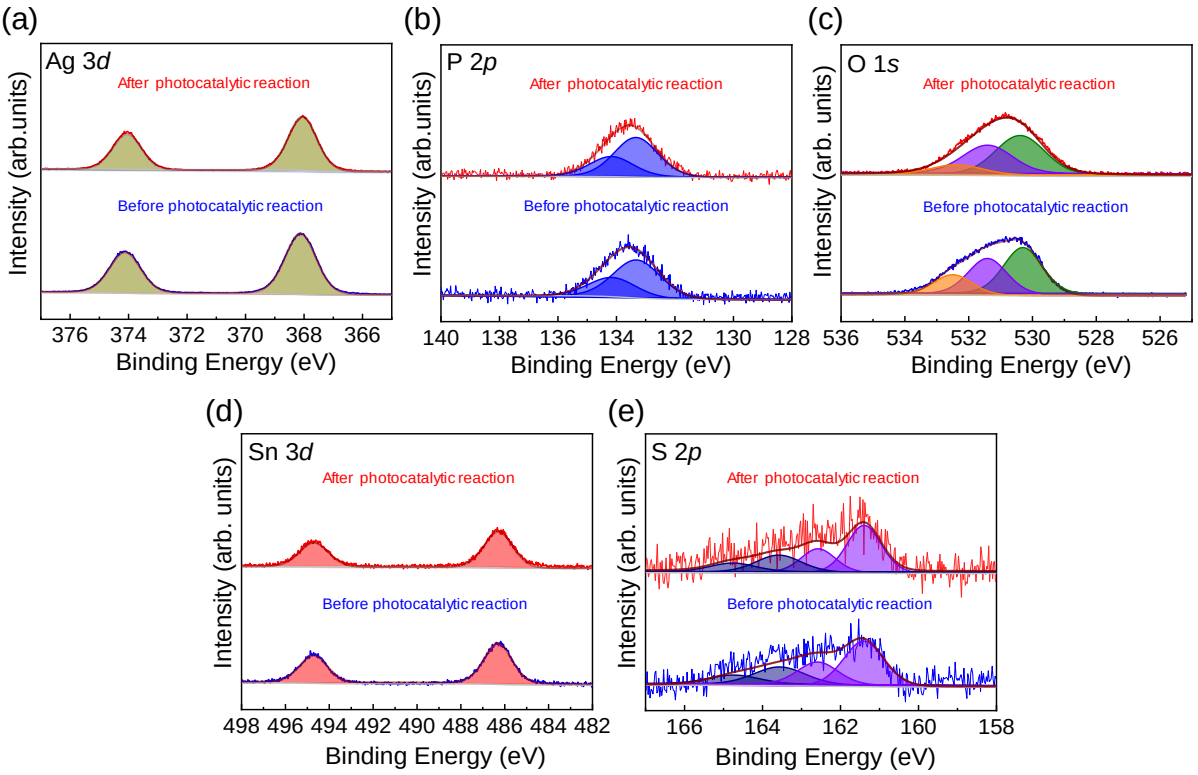

Figure S8. XPS spectra of (a) Ag 3d, (b) P 2p, and (c) O 1s, (d) Sn 3d, and (e) S 2p of Ag_3PO_4/SnS_2 before and after the photocatalytic CO_2 reduction stability test.

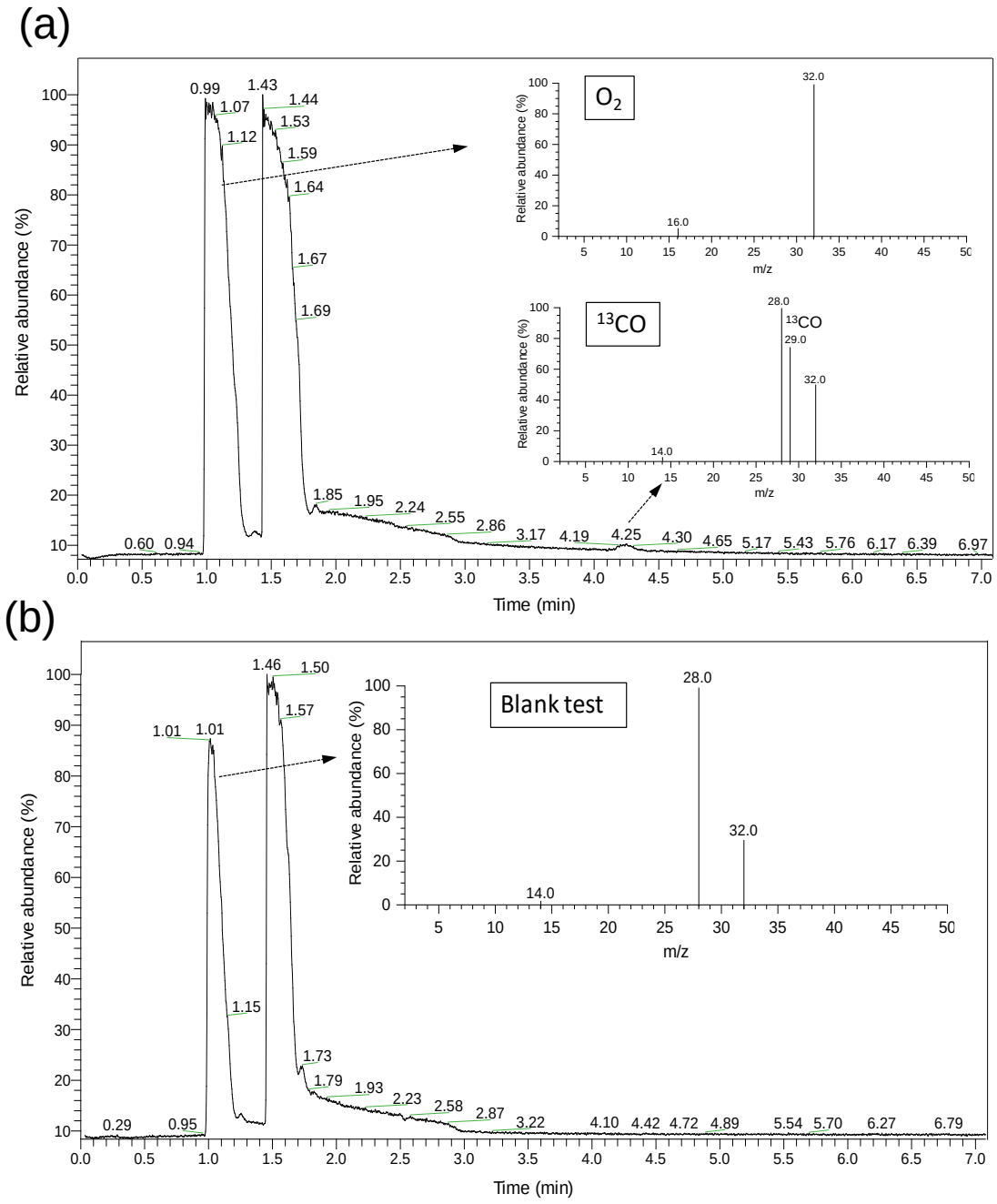

Figure S9. Isotope tracer analysis. Total ion chromatogram and relative mass spectra of (a) isotope tracer $^{13}CO_2$ measurement with O_2 and ^{13}CO detection from photocatalytic CO_2 reduction over Ag_3PO_4/SnS_2, and (b) air blank test measurement over Ag_3PO_4/SnS_2.

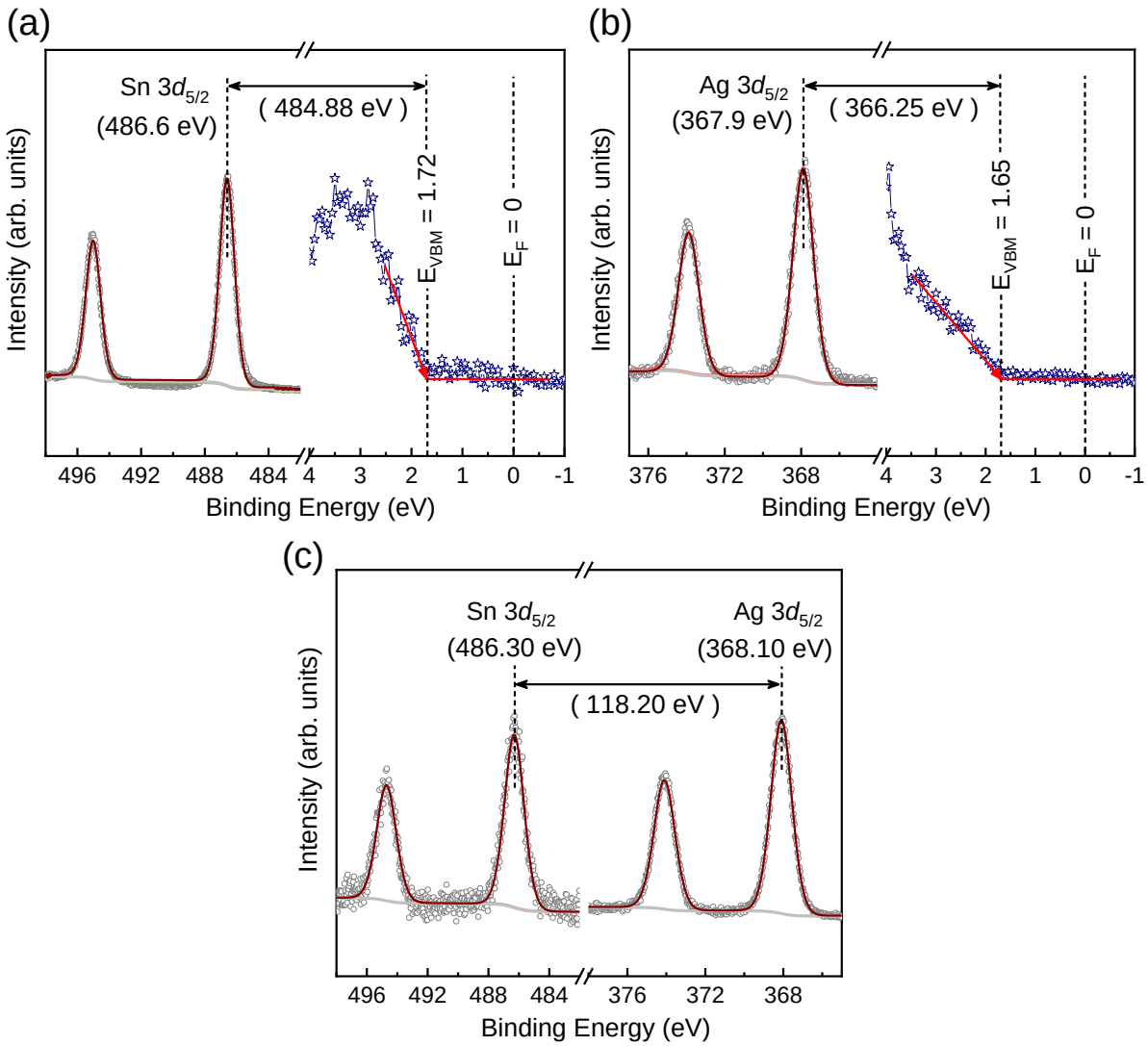

Figure S10. (a) The Sn 3*d* core level and valence band spectra for SnS_2. (b) The spectra of Ag 3*d* core level and valence band for pristine Ag_3PO_4. (c) The spectra of Sn 3*d* and Ag 3*d* core levels for Ag_3PO_4/SnS_2 heterostructure.

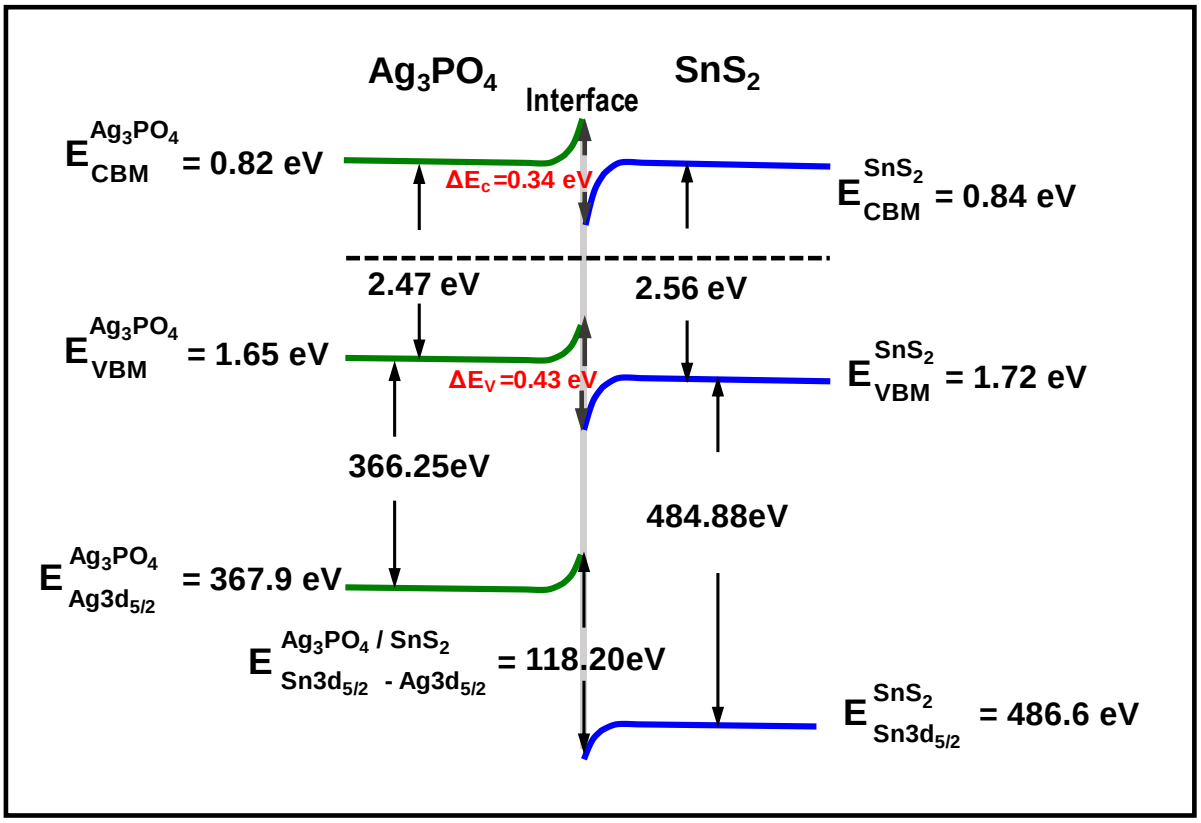

Figure S11. Schematic illustration of band offset at Ag_3PO_4/SnS_2 heterointerface.

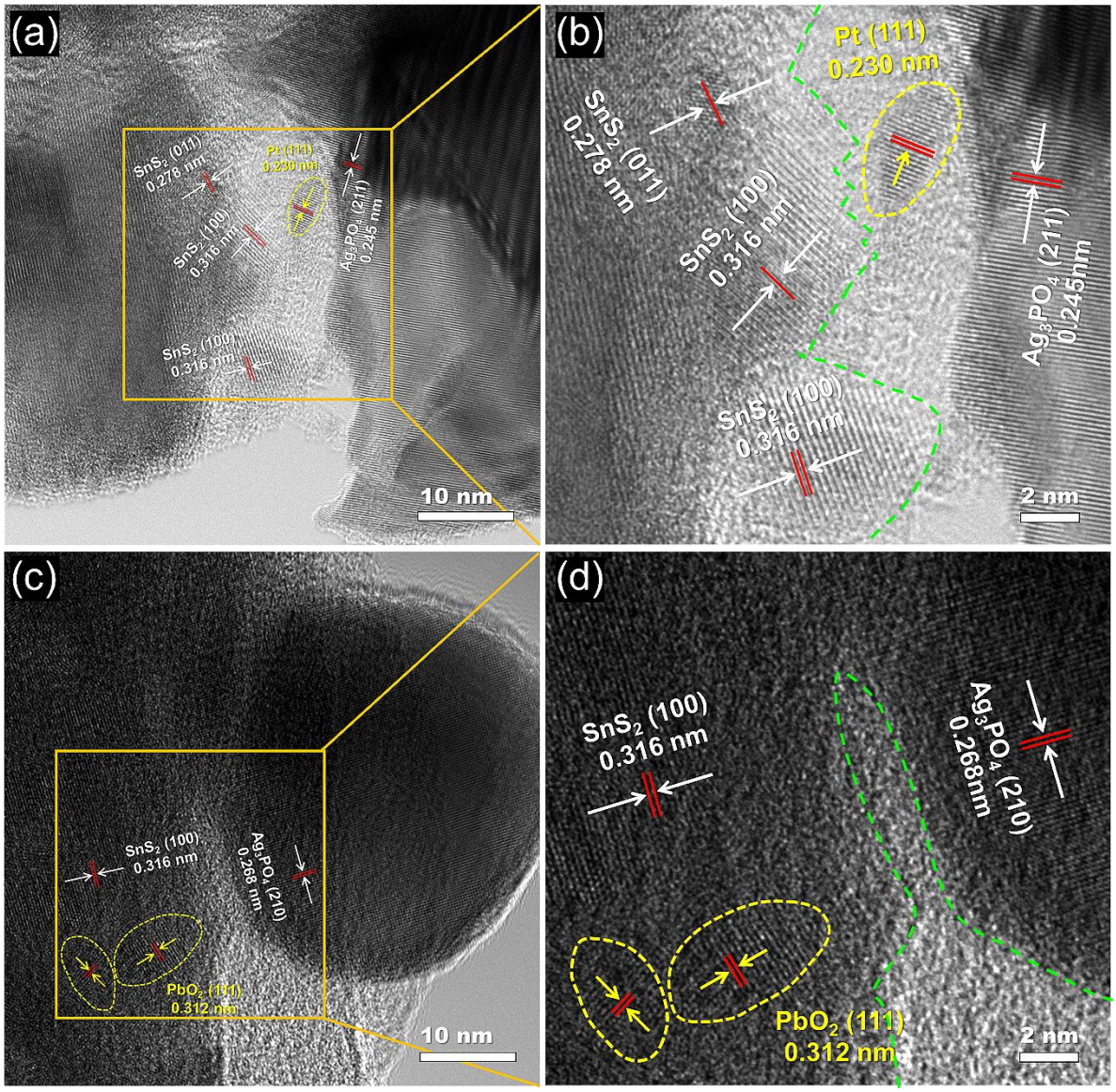

Figure S12. TEM and corresponding HRTEM images after photodeposition of (a–b) Pt and (c–d) PbO_2 nanoparticles on Ag_3PO_4/SnS_2 heterostructure.

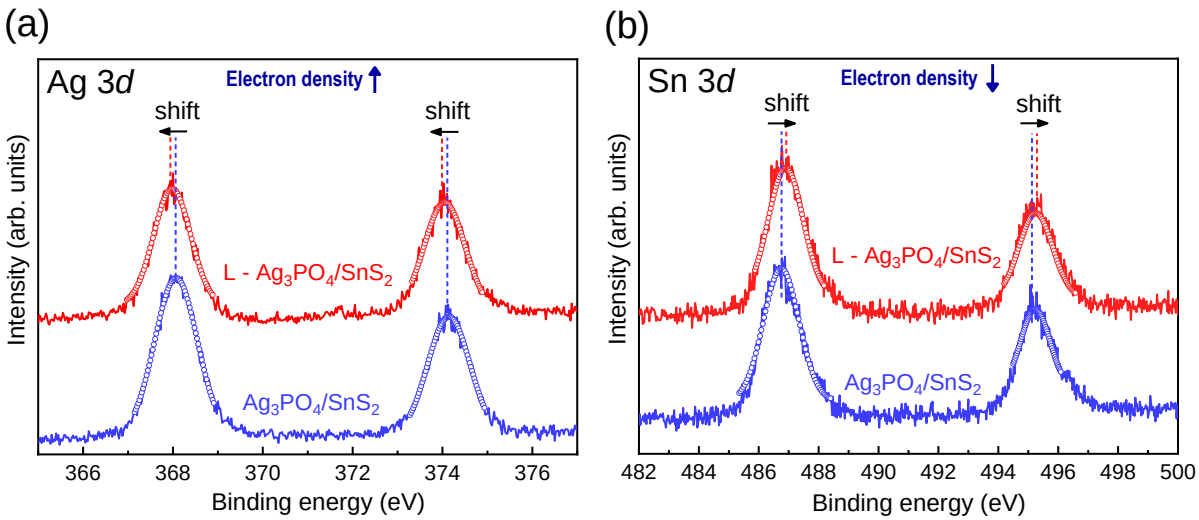

Figure S13. High-resolution XPS analysis for (a) Ag 3d and (b) Sn 3d of Ag_3PO_4/SnS_2 in the dark or under 50 W halogen lamp irradiations.

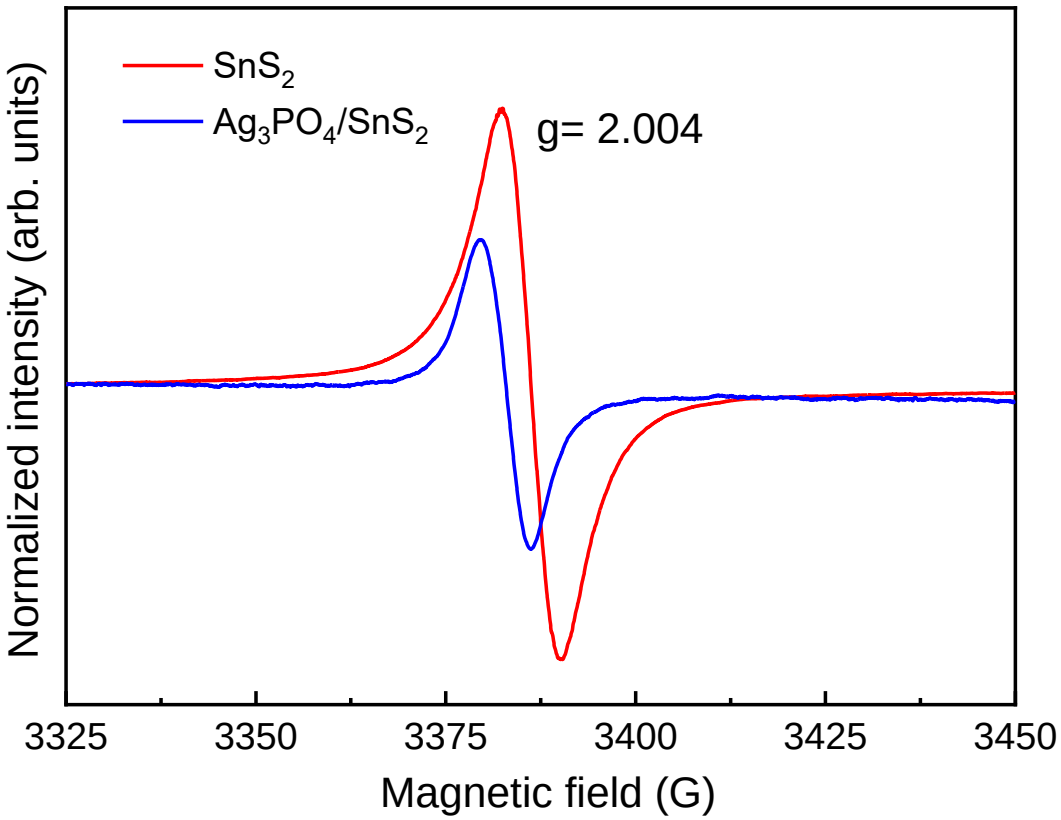

Figure S14. Normalized EPR spectra of SnS_2 and Ag_3PO_4/SnS_2 samples. (The spectra were measured at 77 K in the presence of a vacuum, and the peak intensity has been normalized with the weight of the SnS_2 component in the samples)

Supporting Tables

Table S1. Tabulated elemental analysis of Ag_3PO_4/SnS_2 measured by the XPS. It shows the composition of the orthophosphate semiconductor is $Ag_3\ (PO_{4-x})_{1-y}$ where x = 1.8 and y = 0.15.

Elements	Atomic %
Ag	37.0
P	10.5
O	22.8
Sn	9.9
S	19.8

Table S2. $AQE_{overall}$ of photocatalytic CO_2 reduction over Ag_3PO_4/SnS_2 heterostructure under visible wavelength (400–800 nm)

Light source	Solar simulator (AM1.5)
Photon flux ($cm^{-2}\cdot s^{-1}$)	1.78×10^{17}
CO evolution (μmol)	2.2
Acetaldehyde evolution (μmol)	0.114
Irradiation area (cm^2)	4
Irradiation time (h)	6
$AQE_{overall}$ (%)	0.021

The quantity $AQE_{overall}$ is calculated by the following equation, $AQE_{overall} = \frac{N_e \times (mole\ of\ hydrocarbon\ fuel) \times (6.02 \times 10^{23})}{(Photon\ flux \times Irradiation\ area \times Irradiation\ time)} \times 100\%$ where the N_e is number of reaction electron, and the detail calculation of $AQE_{overall}$ for Ag_3PO_4/SnS_2 heterostructure.

Table S3. The fitting constants of the time-resolved photoluminescence (TRPL) curves recorded at wavelength of 505 nm.

Sample	A_1 (%)	τ_1 (ns)	A_2 (%)	τ_2 (ns)	τ_{ave} (ns)
Ag_3PO_4	52.2	2.45	47.8	10.4	6.25
SnS_2	41.5	0.76	58.5	7.04	4.43
Ag_3PO_4/SnS_2	65.2	0.77	34.8	0.87	0.80

Supporting References

[1] M. Tangi, P. Mishra, C.-C. Tseng, T.K. Ng, M.N. Hedhili, D.H. Anjum, M.S. Alias, N. Wei, L.-J. Li, B.S. Ooi, Band Alignment at GaN/Single-Layer WSe_2 Interface, ACS Appl. Mater. Interfaces 9 (2017) 9110-9117. https://doi.org/10.1021/acsami.6b15370